Stephant et al. (2026)
Exploring nebular ingassing in the inner Solar System: Evidence from the unique achondrite NWA 8409
Advances in Geochemistry and Cosmochemistry 2(1): 764, https://doi.org/10.33063/agc.v2i1.764

Research article

Exploring nebular ingassing in the inner Solar System: Evidence from the unique achondrite NWA 8409

Alice Stephant[1,2] ✉ Steven J. Desch[3] Mahesh Anand[2,4] Xuchao Zhao[2]
Tiberio Cuppone[5] Ben G. Rider-Stokes[2] Cristian Carli[1] Julie Gamblin[6] Evelyn Füri[6]
Mark Nottingham[7] Giovanni Pratesi[5] Ian A. Franchi[2]

[1] Istituto di Astrofisica e Planetologia Spaziali, INAF, Rome, Italy
[2] School of Physical Sciences, The Open University, Milton Keynes, UK
[3] School of Earth and Space Exploration, Arizona State University, USA
[4] Department of Mineralogy, The Natural History Museum, London, UK
[5] Department of Earth Sciences, University of Florence, Italy
[6] Université de Lorraine, CNRS, CRPG, F-54000 Nancy, France
[7] School of Geographical and Earth Sciences, University of Glasgow, UK

✉ **Correspondence to:** A. Stephant: alice.stephant@gmail.com

Author contributions: Conceptualization: AS. Data Curation: AS, XZ, TC, BRS, JG, EF, MN. Formal Analysis: XZ, AS, TC, BRS, JG, EF, MN. Funding Acquisition: AS, MA, GP, CC. Investigation: AS, SJD, MA. Methodology: XZ, AS, TC, BRS, JG, EF, MN. Project Administration: AS. Resources: MA, GP, CC, IAF. Writing – original draft: AS, SJD, MA. Writing – review & editing: All authors.

Data, code, and outputs: https://doi.org/10.5281/zenodo.18949838

Submitted: 2025-04-11
Accepted: 2026-01-05
Published: 2026-03-18

Production editor:
James Darling

Handling editor:
Maitrayee Bose

Reviews:
Two anonymous reviewers

Copyediting:
Elliot Carter,
Marthe Klöcking

The origin of hydrogen in inner Solar System planetesimals remains unknown. Analyses of the hydrogen isotopic composition in non-carbonaceous (NC) chondrites and achondrites can be used as a proxy to determine the origin of this hydrogen. Indeed, the main H reservoirs in the Solar System have distinct isotopic composition. However, NC chondrites and achondrites have yet to reveal the definitive source of their hydrogen. Consequently, it is uncertain whether hydrogen in the parent bodies of these objects originated from outer Solar System sources, such as interstellar ices, or from inner Solar System sources, including nebular gas. The Mercury-like ungrouped achondrite Northwest Africa (NWA) 8409, believed to have formed in the Solar System's innermost regions, offers the unique opportunity to assess nebular H_2 as a potential hydrogen source in planetesimals that formed early and well inward of the snowline. The abundance and isotopic composition of H in nominally anhydrous minerals from NWA 8409 ($\delta D = -560 \pm 166$ ‰) suggest indeed that nebular gas was the principal source of hydrogen in NWA 8409's parent body, supporting the hypothesis that nebular ingassing was a viable process in the early and inner Solar System.

1 Introduction

Over the last few years, several studies have measured the hydrogen (H) isotope composition (δD) and water abundance (a term referring to $H/OH/H_2O$) in a range of achondrites from the non-carbonaceous (NC) reservoir (Kleine et al., 2020; Kruijer et al., 2019), including eucrites (Sarafian et al., 2019; Stephant et al., 2021), angrites (Deligny et al., 2021; Rider-Stokes et al., 2024; Sarafian et al., 2017), acapulcoites-lodranites (Peterson et al., 2024; Stephant et al., 2023), ureilites (Peterson et al., 2023b), aubrites (Peterson et al., 2023a) and some ungrouped achondrites (Newcombe et al., 2023; Tartèse et al., 2019). Such studies aim to answer one of the major unknowns in cosmochemistry, i.e., the source of water to the inner Solar System planetesimals, and by extension, the source of Earth's water (Broadley et al., 2022). Indeed, while water ice was present in the protoplanetary disk beyond the snowline (Morbidelli et al., 2016), as attested by water-rich materials in the carbonaceous reservoir (CC), it remains unclear how the planetesimals that formed inward of the snowline acquired their water (McCubbin and Barnes, 2019; O'Brien et al., 2018). The relevance of hydrogen studies on achondrites and primitive achondrites is that: (i) these meteorites are relics of NC planetesimals that survived the planet formation process and (ii) they accreted only a few

Ma after the calcium-aluminium-rich inclusions (CAIs). As such, NC achondrites and primitive achondrites provide spatial-temporal constraints into the earliest time of the Solar System formation and enable insights to be drawn about the origin of water in early-formed planetesimals that accreted in the inner Solar System.

Two scenarios have been proposed for the source of water in the inner Solar System, involving the two primordial reservoirs of water: interstellar ices and the protosolar nebula gas (Alexander et al., 2012; O'Brien et al., 2018). The first scenario implies that interstellar water ices (Cleeves et al., 2014) could have been incorporated similarly to how parent bodies of carbonaceous chondrites (CCs) acquired water, either as ice grains originating in the molecular cloud and feeding the protoplanetary disk (Piani et al., 2021) or carried by components such as ice-mantled chondrules (Ciesla et al., 2003). Alternatively, water vapor could react with silicates in the nebula, producing hydrogen-bearing phyllosilicates (Kalyaan and Desch, 2019; Marrocchi et al., 2023). This scenario practically requires that this water reservoir (and the water snowline) existed inside Jupiter's orbit before the separation of the NC and CC reservoirs by the formation of Jupiter. Another way to deliver water to the NC region involves the influx of water-rich bodies by planetesimal scattering during the growth of the giant planets (Raymond and Izidoro, 2017). However, while this later volatile delivery is highly favoured for the origin of Earth's volatiles, it fails to reconcile the origin of water in NC differentiated planetesimals, which have accretion ages older than that of CC's parent bodies (Desch et al., 2018; McCubbin and Barnes, 2019).

The second, more debated scenario, implies that water was sourced only locally (Drake, 2005). H_2 gas from the nebula could have been acquired in an isotopically fractionated manner by grain-scale processes such as adsorption (Asaduzzaman et al., 2015) or protoplanetary-scale processes such as ingassing (Olson and Sharp, 2018; Wu et al., 2018; Yang et al., 2016). Both scenarios are subject to dynamical and cosmochemical constraints (O'Brien et al., 2018), and deciphering which is the favoured process will help to better constrain the Solar System formation and evolution, as well as infer volatile distribution in exoplanetary systems. The search for Earth's volatiles has led to the current understanding that both scenarios must have played a role in contributing to the Earth's volatile budget, meaning that hydrogen would have been sourced both locally and delivered by the outer Solar System bodies (Broadley et al., 2022). However, because of its large size and its long and complex history, the Earth is not considered representative of the inner Solar System planetesimals. As such, achondrites and primitive achondrites hold the key to understanding the origin of in-situ volatiles in the inner Solar System.

So far, it has been estimated that all NC achondrite and primitive achondrite parent bodies contain low but significant bulk water contents (e.g., 2–110 µg/g H_2O), associated with a similar hydrogen isotopic composition, expressed in δD value of −250 ± 50 ‰ (Deligny et al., 2021; Peterson et al., 2024, 2023a,b; Rider-Stokes et al., 2024; Sarafian et al., 2019, 2017; Stephant et al., 2023, 2021). Studies measuring bulk and nominally anhydrous minerals in ordinary chondrites (OCs), also formed in the NC reservoir, find similarly this low δD signature (Chan et al., 2021; Grant et al., 2024; Jin et al., 2021). One should note that heavier δD measured in chondrules (> 10 000 ‰) have been assigned to a secondary origin (Shimizu et al., 2021). These recent results have been taken as evidence for the presence of a pervasive and unique source of water in the inner Solar System planetesimals within the first 10 Myr after CAI formation, in which the hydrogen isotopic ratio is slightly lower than the bulk CCs (Rider-Stokes et al., 2024; Stephant et al., 2023).

The hydrogen isotope ratio in water is considered to be diagnostic of its source in the Solar System, with interstellar ices having elevated δD values > +9000 ‰ (Dartois et al., 2003) and the protosolar nebula being highly depleted in D (i.e., δD value of −897 ‰; Gloeckler and Geiss, 1998); however, either primordial source could theoretically reach δD values similar to those measured in NC achondrites, through various fractionation pathways (Marrocchi et al., 2023; Olson and Sharp, 2018; Piani et al., 2021; Wu et al., 2018). This results in difficulty identifying the unique source of hydrogen in these parental bodies. In fact, it is likely a combination of these sources. Isotopic exchange between water vapor produced by the sublimation of D-rich ice, and protosolar H_2 gas can also lead to a δD value of −250 ± 50 ‰ (Lécluse and Robert, 1994). Indeed such a process has been suggested to have formed a common D-poor water background reservoir in the inner and outer Solar System, based on δD similarity between unequilibrated OCs and CCs ices (Grant et al., 2024). Currently, it seems that nebular H_2 contributed to the isotopic ratios of NC samples, but indirectly, through gas-phase equilibration between H_2 and H_2O vapor. It is not clear whether any NC samples directly incorporate nebular H_2.

Northwest Africa (NWA) 8409, paired with NWA 7325, NWA 8014, NWA 8486, and other stones from the Bir Abbas site (see Meteoritical Bulletin), is a unique ungrouped achondrite characterized by a reduced, FeO-poor composition and gabbroic texture, which may have formed through an impact melting event at high temperatures and low oxygen fugacity, approaching enstatite-rich meteorite conditions (Barrat et al., 2015; Goodrich et al., 2017; Irving et al., 2013; Yang et al., 2020). Notably, NWA 8409 and its paired achondrites were initially hypothesized to be fragments of Mercury due to their unique chemical compositions (Irving et al., 2013; Sutton et al., 2017). However, this theory has since been questioned based on inconsistencies, such as differences in spectral reflectance (Cloutis et al., 2018). Furthermore, the onset of differentiation for the parent bodies of these meteorites is estimated to have occurred 1.72–1.80 Ma after CAIs (Koefoed et al., 2016; Yang et al., 2020), suggesting that NWA 8409 may represent one of the earliest crusts of a differentiated planetesimal, predating Mercury per se. Nevertheless, it was suggested that NWA 7325 (and paired meteorites) could be derived from daughter bodies produced by a mantle-stripping impact on proto-

Mercury (Desch et al., 2022), which would align with the hypothesis that these meteorites formed through a shock-induced melting event (Yang et al., 2020). Thus, it is possible these meteorites contain ingassed nebular H_2 and could provide crucial insights into the sources of hydrogen in the innermost Solar System. In this study, we analyse the hydrogen abundance and isotope composition (expressed as H_2O contents and δD ratios) of nominally anhydrous minerals (NAMs) in NWA 8409. Our objective is to trace the sources of hydrogen in bodies that accreted within the Solar System's innermost regions, thereby contributing to our understanding of the processes that led to water incorporation in the early inner Solar System planetesimals, and, ultimately, the Earth.

2 Methods

2.1 Petrography and chemistry

Preliminary petrographical and mineralogical characterization through Scanning Electron Microscopy (SEM) imaging, as well as semi-quantitative micro-chemical analyses, were obtained at MEMA (Centro Servizi di Microscopia Elettronica e Microanalisi) at the University of Firenze (Italy) using a SEM-EDS (ZEISS EVO MA 15) equipped with an EDS/SDD analytical system, an Oxford Ultimax 40 detector and the Aztec 5.0 SP1 software. Chemical characterization of silicates and sulfides on NWA 8409 chip were carried out at the joined laboratory (LaMA, Laboratorio MicroAnalisi) of the Earth Sciences Department of the University of Firenze (DST) and the National Council of Research - Institute of Geosciences and Earth Resources (CNR-IGG) of Firenze. The determinations of bulk major and trace element compositions were performed at the Department of Earth Sciences, University of Firenze. For petrographic examination, the small chip of NWA 8409 was investigated using a FIB-SEM Zeiss Crossbeam 550 at The Open University (UK) fitted with an Oxford Instruments Symmetry 2 Electron Back-Scattered Detector (EBSD). Details for all these methods can be found in Supplementary Material.

2.2 Noble gases

The noble gas (Ne and Ar) abundances and isotope ratios of two bulk rock fragments (5.53 and 6.32 mg) of NWA 8409 were analysed at the noble gas facility of the Centre de Recherches Pétrographiques et Géochimiques (CRPG, France). The samples were placed into a ZnSe-windowed laser chamber, which was pumped to ultra-high vacuum (~10^{-9} bar). Overnight baking at ~100 °C allowed adsorbed terrestrial gases to be removed from the internal surfaces of the laser chamber and the samples. The gases of interest were extracted under static vacuum using a 10.6 µm CO_2 laser (MIR102, Elemental Scientific). The first sample was heated for 3 min at the maximum laser power of 32 W. The second sample was heated more gradually to avoid spattering caused by vigorous bubbling that occurred upon melting, reaching 70 % of the maximum laser power after 3 min. It was then heated a second time for 3 min at maximum laser power. In both cases, all noble gases are expected to have been extracted. Argon was first separated from Ne by adsorption onto a charcoal finger held at −196 °C using liquid nitrogen for 5 min. The two noble gases were then successively purified in an all-metal purification line using a Ti-sponge getter heated to 600 °C for 10 min and two GP-50 SAES getters at room temperature for 10 min. To enhance Ne purification, a second charcoal finger maintained at liquid nitrogen temperature was employed. The purified gases were sequentially analysed using a NoblesseHR noble gas mass spectrometer in multi-collection mode, with at a trap current of 150 µA and source settings optimized for each species to maximize sensitivity and minimize instrumental mass fractionation (Zimmermann et al., 2025). The three Ne isotopes were analysed simultaneously on three ion counters ($^{22}Ne^+$ on IC0, $^{21}Ne^+$ on IC2, $^{20}Ne^+$ on IC3) for 25 cycles. The contributions of doubly charged $^{40}Ar^{++}$ and $^{44}CO_2{}^{++}$ to the $^{20}Ne^+$ and $^{22}Ne^+$ signals, respectively, were minimized by employing a charcoal finger held at −196 °C and two GP-50 SAES getters, connected to the source and detector blocks, for 10 min prior to the start of the analysis and during the analytical sequence. No $^{40}Ar^{++}$ correction was applied to the $^{20}Ne^+$ signal as the two peaks were partially resolved. Additionally, no $^{20}NeH^+$ hydride correction was applied to the $^{21}Ne^+$ signal as the getters maintained a low H_2 background. The $^{44}CO_2{}^+$ signal was monitored during the analyses, and the $^{44}CO_2{}^{++}$ contribution was corrected from the $^{22}Ne^+$ signal using a $^{44}CO_2{}^{++}/{}^{44}CO_2{}^+$ ionization ratio of 1.2 %, although it was negligible (< 2 cps). The three Ar isotopes were analysed simultaneously on two ion counters and a Faraday detector ($^{40}Ar^+$ on Fa0 with a 10^{11} Ω resistor, $^{38}Ar^+$ on IC2, $^{36}Ar^+$ on IC3) for 25 cycles. During the Ar analysis, two GP-50 SAES getters were used to maintain a constant, low H_2 level and to minimise the $H^{35,37}Cl^+$ signals. All measured ion signals were corrected for the detector baselines. Noble gas abundances and isotope ratios were calculated based on the sensitivity and instrumental mass fractionation of the mass spectrometer and corrected for blank contributions. The analytical sensitivity and instrumental mass fractionation were estimated using air aliquots analysed before and during the measurement period. The reproducibility of air standard measurements was 1.88 % for ^{21}Ne, and 1.23 % for ^{38}Ar abundances, and 0.25 % for $^{20}Ne/^{22}Ne$, 1.64 % for $^{21}Ne/^{22}Ne$, and 0.44 % for $^{38}Ar/^{36}Ar$ isotope ratios. Procedural blanks averaged 3.7×10^{-19} mol ^{21}Ne and 1.8×10^{-18} mol ^{38}Ar.

2.3 H concentration and isotope

Secondary ion mass spectrometry (SIMS) measurements of D/H ratios and H_2O concentrations in six pyroxenes and six olivines were performed with the Cameca NanoSIMS 50L at The Open University following established protocols (Stephant et al., 2023). For nominally anhydrous minerals, H^-, D^-, $^{13}C^-$ and $^{16}O^-$ secondary ions were measured using electron multipliers ($^{16}O^-$ on Faraday cup) using a Cs^+ primary beam of ~2 nA rastered over a 10 µm × 10 µm

surface area. The electron gun was tuned to an electron current of approximately 5 µA. Analysis of $^{13}C^-$ was used to monitor any potential terrestrial contamination and presence of cracks. Large and flat NAMs were selected for analysis. Blanking was performed, and only the 4 µm × 4 µm (16 %) interior of the surface area was analysed, with each measurement consisting of 2000 cycles of ~0.54 s each, providing a total analysis time of ~20 min. Prior to the analysis, an area of 12 µm × 12 µm was pre-sputtered for ~10 min using the same primary beam current. The vacuum in the analytical chamber was around 2.0×10^{-10} Torr.

The H_2O contents in nominally anhydrous minerals were determined using a $H^-/^{16}O^-$ vs. H_2O calibration based on terrestrial orthopyroxenes for olivine (Supplementary Fig. S1) and terrestrial clinopyroxenes for high-Ca pyroxenes (Supplementary Fig. S2, Table S1 Kumamoto et al., 2017). Indeed, it has been shown that our orthopyroxene reference materials can also be used to measure water in olivine based on observations that these two minerals have similar calibration slopes (Kumamoto et al., 2017). The nominally anhydrous San Carlos olivine (SCOL) was used as a blank to estimate the $H^-/^{16}O^-$ (Fig. S3) and D^-/H^- (Fig. S4) background in the analytical chamber, before and after sample analyses, in order to correct appropriately the unknowns. All standards and the meteorite were mounted in indium. SCOL and NWA 8409 were mounted in the same mount. The H_2O background during NAMs session ($H^-/^{16}O^-$ background = $(2.47 \pm 0.16) \times 10^{-7}$; Fig. S3) corresponds to a water content of 1.10 ± 0.07 µg/g. It is interesting to note that the $H^-/^{16}O^-$ background estimated from SCOL matches the intercept of $H^-/^{16}O^-$ vs. H_2O calibration lines (Figs S1 and S2). The background-corrected detection (BLOD) limit of H_2O is estimated to be 0.21 µg/g H_2O, as defined as three times the uncertainty (1 SD) of the analytical background (e.g., Peterson et al., 2024).

The measured D/H ratios are expressed in terms of δD values, defined as follows:

$$\delta D = [(D/H)_{sample}/(D/H)_{VSMOW} - 1] \times 1000$$

where $(D/H)_{VSMOW} = 155.76 \times 10^{-6}$. Pyroxene KBH-1 (see Table S1) was measured to estimate the instrumental mass fractionation (IMF = 1.11 ± 0.01, 2SD, n = 5). Once corrected from IMF, the unknowns were corrected for background contamination using SCOL (Fig. S4; $\delta D_{background} = -127 \pm 141$ ‰) and spallation production using cosmic exposure age of sample estimated in this study (i.e., 17.5 ± 0.5 Ma). Errors estimated for H_2O concentrations are 2SD and take into account the errors from counting statistics and the 2SD of San Carlos analyses. Errors estimated for δD values are 2SD and take into consideration the errors based on counting statistics, as well as the errors associated to the IMF determination and on the background δD value. Repeatability of $\delta D_{background}$ is < 13 %.

Table 1. Modal abundances and major chemical composition of phases in NWA 8409.

Mineral	Modal abundance %	n	SiO_2 wt%	TiO_2 wt%	Al_2O_3 wt%	Cr_2O_3 wt%	FeO wt%	MnO wt%	MgO wt%	CaO wt%	Na_2O wt%	K_2O wt%	Total wt%	Endmembers
Pyroxene	40.8	13	53.63	0.06	2.84	0.97	0.52	0.03	19.07	22.09	0.17	0.001	99.38	$En_{54.1}Wo_{45.1}Fs_{0.8}$
1SD			0.33	0.01	0.04	0.02	0.03	0.01	0.11	0.11	0.01	0.003	0.35	
Plagioclase	51.4	7	45.61	0.02	34.69	-	0.04	<0.003	0.41	17.53	1.13	0.01	99.44	$An_{89.5}Ab_{10.5}$
1SD			0.53	0.01	0.66	-	0.03	0.01	0.38	0.42	0.10	<0.001	0.30	
Olivine	4.5	8	41.69	0.02	0.04	0.34	2.05	0.07	55.11	0.37	-	-	99.69	$Fo_{97.95}$
1SD			0.56	0.01	0.01	0.04	0.07	0.02	0.43	0.04	-	-	0.41	

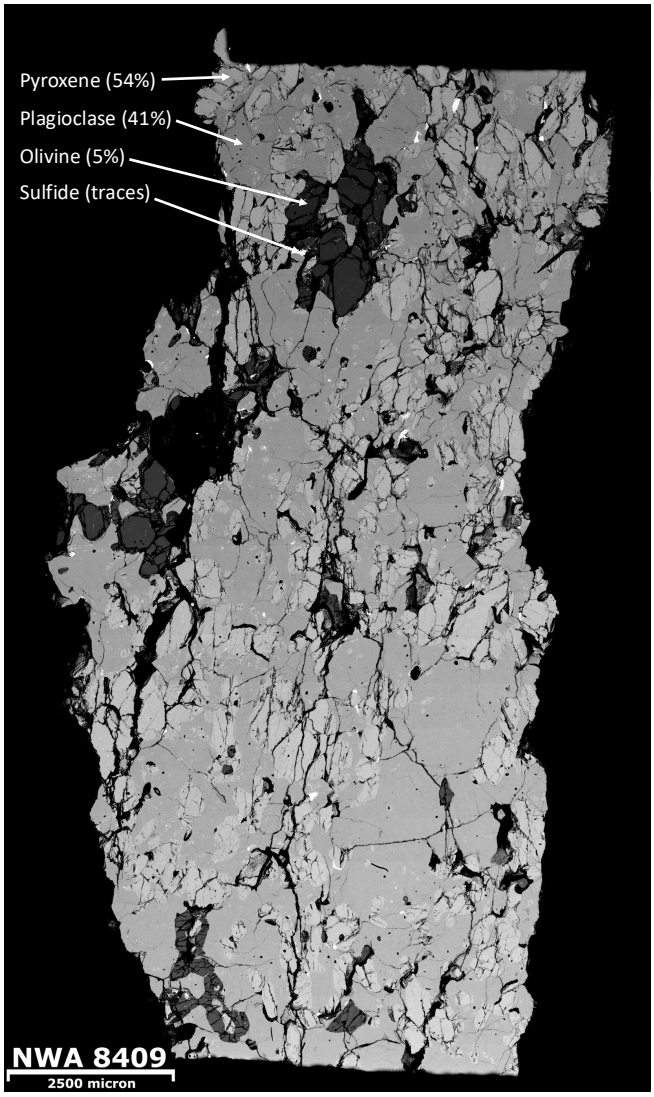

Figure 1. BSE map of the NWA 8409 chip analysed in this study. Modal abundances of pyroxene, plagioclase, olivines and sulfides are reported here.

3 Results

3.1 Petrography and geochemistry

Our large chip (2 cm × 0.9 cm × 0.5 cm) of NWA 8409 (Figure 1) contains 54 vol % of calcic plagioclase ($An_{89.5\pm1.0}$ $Ab_{10.5\pm1.0}$), 41 vol % of diopside ($En_{54.1\pm0.2}$ $Wo_{45.1\pm0.2}$ $Fs_{0.8\pm0.1}$), 5 vol % of forsteritic olivine ($Fo_{97.8\pm0.1}$) and traces of sulfides (Table 1). Modal abundance heterogeneity has been observed amongst the various NWA 7325 sections studied (Barrat et al., 2015; Bischoff et al., 2013; Goodrich et al., 2017; Weber et al., 2016; Yang et al., 2020). Indeed, olivine, pyroxene and plagioclase modal abundances range between 2–15 vol %, 25–44 vol % and 51–60 vol %, respectively. NWA 8486 presents much lower modal abundance of olivine (4 vol %), similar to NWA 8409, lower plagioclase modal abundance (44 vol %) and higher pyroxene modal abundance (52 vol %) (Frossard et al., 2019). As such, our studied chip of NWA 8409 resembles the NWA 7325 section studied by Weber et al. (2016). The large variation in olivine modal abundance in NWA 7325 could be easily explained by the fact that olivine is present in clusters (Figure 1). In terms of chemical composition, minerals present in NWA 8409 are in the range of NWA 7325 compositions, with a slightly more forsteritic olivine ($Fa_{2.05\pm0.07}$, $Fo_{97.95\pm0.07}$; Cr_2O_3 = 0.34±0.04; CaO=0.37±0.04). Pyroxene and plagioclase chemical compositions ($En_{54.11\pm0.18}$ $Wo_{45.06\pm0.19}$ $Fs_{0.82\pm0.04}$ and $An_{89.49\pm1.02}$ $Ab_{10.48\pm1.03}$ $Or_{0.05\pm0.02}$, respectively) are within the range of previous studies of both NWA 7325 and NWA 8486, with $En_{49\text{-}56}$ $Wo_{39.5\text{-}46.0}$ and $An_{79\text{-}94.}$ The REE pattern is extremely similar between NWA 7325 and NWA 8409, as well as their bulk composition (Figures S5 and S6; Supporting Data, Stephant et al., 2026). The only discrepancy is the slight enrichment in light REE which could be explained by slight contamination during terrestrial residence, or during the cutting of the chip, as suggested by Barrat et al. (2015) for dust analyses of NWA 7325 (cf. Irving et al., 2013).

Previous studies have highlighted some noble gases heterogeneities in NWA 7325, resulting in a ~4 Ma variation of the cosmic ray exposure ages (CRE). Indeed, two studies reported similar CRE ages of 17.45 ± 0.12 Ma (Hopp et al., 2018) and 18.8–18.9 Ma (Weber et al., 2016). However, Hopp et al. (2018) argued that using their calculation method on the data of Weber et al. (2016), the CRE age will decrease to 13.5–14 Ma, highlighting some potential noble gases heterogeneities. To best correct for D produced by spallation, noble gases analyses have been performed on our analysed chip. Ne and Ar isotopes, together with $^{20}Ne/^{22}Ne$, $^{21}Ne/^{22}Ne$, $^{40}Ar/^{36}Ar$ and $^{38}Ar/^{36}Ar$, are reported in Table 2.

We applied the chemistry of NWA 8409 to the theoretical cosmogenic nuclide production rate models of Leya and Masarik (2009). The resulting model, as seen in Figure S7a, shows that the Ne isotopic inventory of NWA 8409 is consistent with a pure cosmogenic composition. However, it is apparent, by way of the different total inventory isotopic ratios of the two aliquots measured, that the sample-specific chemistries of each aliquot differ (see Figure S7b). This is also reflected in Figure S8, by the two measurements not converging on a single set of burial conditions. This is likely due to inconsistent sampling of each mineral type between the two measured aliquots, due to the coarse-grained nature of the sample, resulting in aliquot-specific chemical heterogeneity. It is highly unlikely that the two aliquots experienced significantly different cosmic ray exposure conditions (i.e. burial depths).

A requirement for these theoretical cosmogenic nuclide production rate models is the assumption of a meteoroid size and sample burial depth. This parameter accounts for the changes in the particle fluxes a sample is exposed to, as the flux exposure geometry varies from a spherical 4π isotropic vector field, to a hemispherical 2π anisotropic vector field (see Figure S9). We would expect each measured $^{21}Ne/^{22}Ne$ isotopic ratio (which varies primarily due to differences in possible nuclear pathways of Mg isotopes to produce Ne isotopes) to intersect with their sample-specific

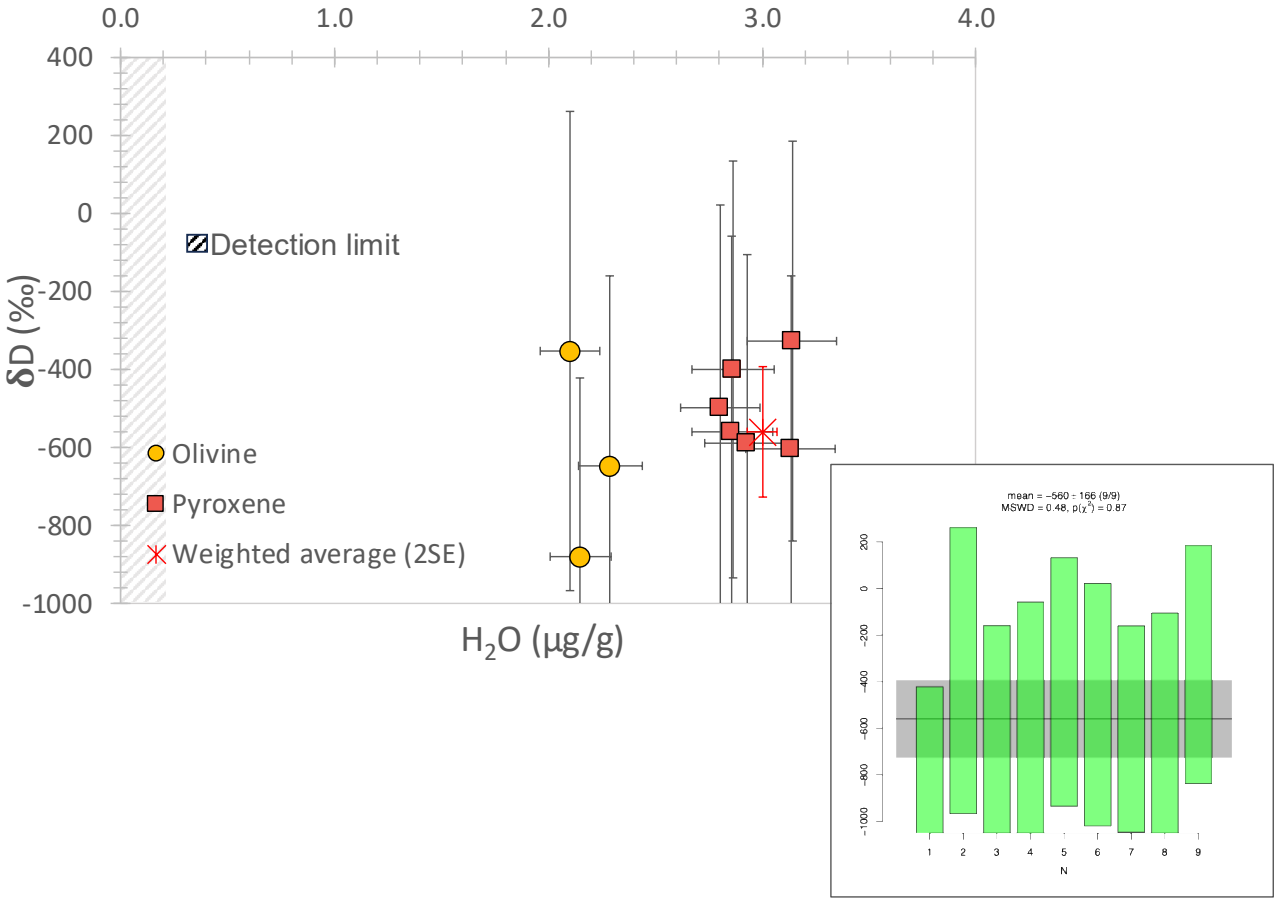

Figure 2. Hydrogen isotope composition and abundance in NWA 8409 pyroxenes. δD is expressed in ‰ and H_2O contents in µg/g of olivine (yellow circles) and pyroxene (orange squares) in NWA 8409. The error bars are 2 s.d. uncertainties (see Supporting Data, Stephant et al., 2026). The weighted mean δD of NWA8409 is represented as an orange cross (δD = −560 ± 166 ‰, n = 9, 2SE). An inset shows the weighted mean and 2SE, with the MSWD and the P value of the Chi square (IsoplotR; Vermeesch, 2018).

chemistry-representative theoretical cosmogenic nuclide production rate ratio curve, with both aliquot measurements converging on one set of shielding conditions, represented in these curves.

Based on the poor fit of both aliquots to a singular set of burial conditions using the applied chemistry from the literature, it is impractical to calculate a precise cosmic ray exposure age. However, by modelling the resulting cosmic ray exposure age of a range of burial conditions, within the limits of the model of Leya and Masarik (2009), we estimate a minimum exposure age of 17.5 ± 0.5 Ma, which corresponds to a burial depth of 48–49 cm within a meteoroid of 65 cm radius. We note that this is consistent with the ages calculated by previous studies (Hopp et al., 2018; Weber et al., 2016).

3.2 NanoSIMS

Olivine water content ranges from 1.5 ± 0.1 to 2.3 ± 0.2 µg H_2O/g (2SD), respectively (Figure 1; Table 3). This prevents any reliable estimate of an associated δD value for olivine with a H_2O content below 2 µg H_2O/g, for the three other olivines, δD value ranges from −878 ± 551 (2SD) to −352 ± 767 ‰ (2SD). Pyroxenes water content range between 2.9 ± 0.2 to 3.1 ± 0.2 µg H_2O/g (2SD), with δD value ranging from −601 ± 443 (2SD) to −324 ± 512 ‰ (2SD) (Figure 2; Table 3), after careful instrumental mass fractionation (IMF) correction, background correction and spallation correction (Table 3). All these corrections and associated errors have been calculated based on standard measurements (see Supporting Data, Stephant et al., 2026). Our Ne isotopic analyses of the same piece of NWA 8409 where D/H analyses were performed, are consistent with a CRE age of 17.5 ± 0.5 Ma, which has been determined for the paired sample NWA 7325 (Hopp et al., 2018). Olivine and pyroxene in NWA 8409 are minimally strained from shock and show no signs of recrystallization (Supplementary Figure S9), consistent with the assigned S2 shock stage of NWA 7325 (Bischoff et al., 2013). As such, H should not have been affected. As the shock and associated melting would have led to devolatilization, implying both higher initial H_2O content and lower initial δD, these δD values

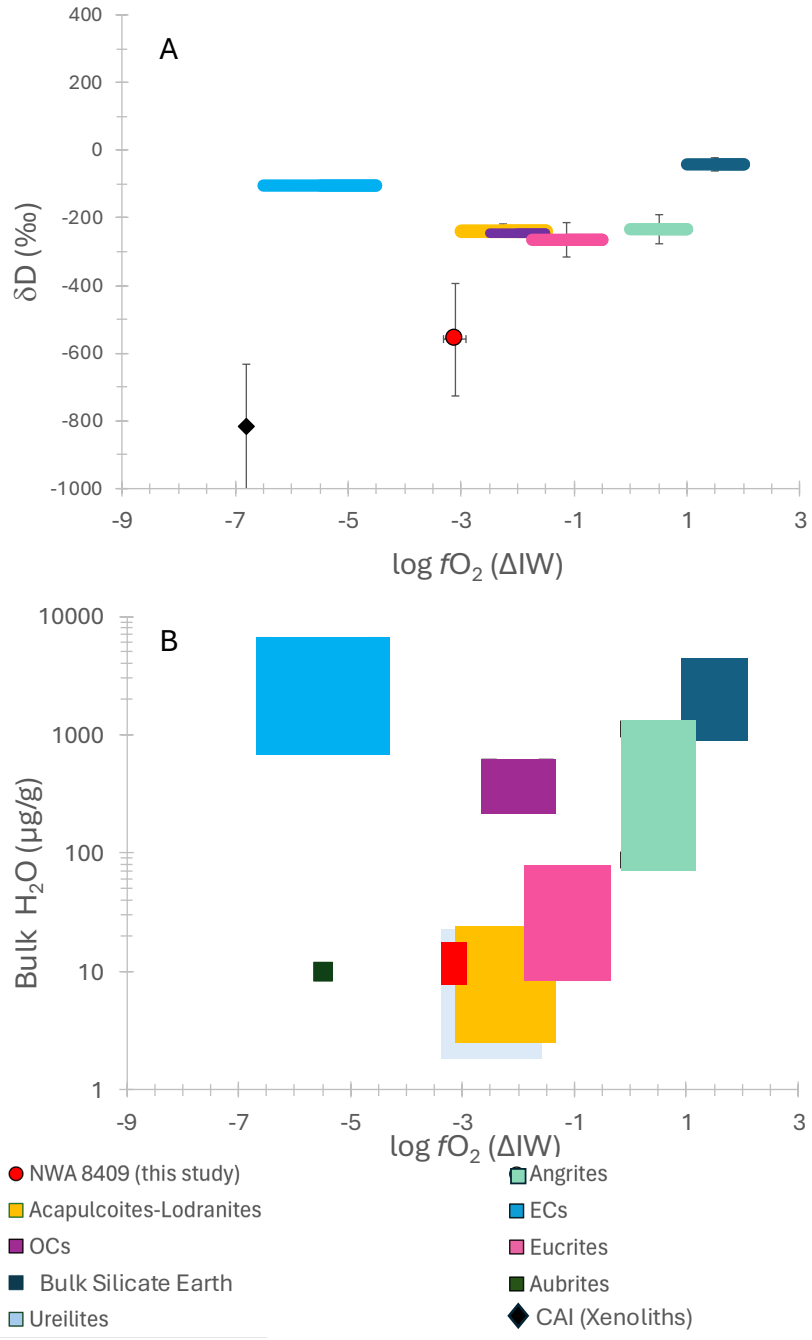

Figure 3. Oxygen fugacity (log fO2 (ΔIW)) vs. δD (in ‰) (A) and vs. bulk H_2O (in µg/g) (B) in chondrites, achondrites and primitive achondrites from the NC reservoir. Literature data have been used for acapulcoites-lodranite (Stephant et al., 2023), OCs (Jin et al., 2021), bulk silicate Earth (Lécuyer et al., 1998; Peslier et al., 2017), ureilites (Peterson et al., 2023b), CAI (Aléon et al., 2022), angrites (Rider-Stokes et al., 2024), ECs (Piani et al., 2020), eucrites (Stephant et al., 2021), aubrites (Peterson et al., 2023a) and UOCs (Grant et al., 2024).

can be seen as upper limits for the Mercury-like NWA 8409 parent body.

Raw data of standards and NWA 8409 NAMs, as well as detailed data correction can be found in Supporting Data (Stephant et al., 2026).

3.3 Reliability of the data

Newcombe et al. (2023) have found no detectable water in NWA 8409. However, (i) they only performed three analyses distributed in two pyroxene grains and (ii) their water content background was higher than in this study, i.e. 3.34 µg/g H_2O. As such, considering that we measured 3 µg/g H_2O with a lower background of 1.1 µg/g, there is no significant difference between these studies, but a better detection limit in our analyses. Because of the very low water contents in both olivine and pyroxenes of NWA 8409, the magnitude of the corrections between the analysed δD and the final spallation corrected δD is large, which may raise

Table 2. Noble gases Ne and Ar isotope abundances, together with $^{20}Ne/^{22}Ne$, $^{21}Ne/^{22}Ne$, $^{40}Ar/^{36}Ar$ and $^{38}Ar/^{36}Ar$

Sample	Mass	^{20}Ne	±	^{21}Ne	±	^{22}Ne	±	$^{20}Ne/^{22}Ne$	±	$^{21}Ne/^{22}Ne$	±
	mg	10^{-12} mol g^{-1}	10^{-14} mol g^{-1}	10^{-12} mol g^{-1}	10^{-14} mol g^{-1}	10^{-12} mol g^{-1}	10^{-14} mol g^{-1}				
NWA 8409 #1	5.53	2.39	1.66	2.55	4.79	2.97	2.41	0.80	0.02	0.8615	0.0142
NWA 8409 #2 (1/2)	6.32	2.09	1.45	2.18	4.10	2.66	2.16	0.78	0.02	0.8239	0.0136
NWA 8409 #2 (2/2)	6.32	0.15	0.19	0.13	0.25	0.16	0.13	0.96	0.03	0.8475	0.0139
NWA 8409 #2	6.32	2.25	1.47	2.31	4.11	2.82	2.16	0.80	0.02	0.8252	0.0128

Sample	Mass	^{40}Ar	±	^{38}Ar	±	^{36}Ar	±	$^{40}Ar/^{36}Ar$	±	$^{38}Ar/^{36}Ar$	±
	mg	10^{-11} mol g^{-1}	10^{-13} mol g^{-1}	10^{-12} mol g^{-1}	10^{-14} mol g^{-1}	10^{-12} mol g^{-1}	10^{-14} mol g^{-1}				
NWA 8409 #1	5.53	2.15	1.79	0.69	0.85	0.52	0.45	41.46	0.27	1.317	0.006
NWA 8409 #2 (1/2)	6.32	2.27	1.88	1.51	1.87	1.06	0.90	21.58	0.27	1.433	0.006
NWA 8409 #2 (2/2)	6.32	0.31	0.31	0.24	0.30	0.17	0.14	19.02	0.29	1.459	0.006
NWA 8409 #2	6.32	2.58	1.91	1.75	1.89	1.23	0.91	21.27	0.24	1.436	0.006

questions regarding the reliability and the credibility of the data. It is worth emphasizing that the spallation correction was made using the well-established production rates of D from Füri et al. (2017), as routinely applied in other D/H studies, and a cosmic-ray exposure (CRE) age re-evaluated in this study that remains consistent with previous estimates for paired samples. Therefore, although the spallation correction induces a large absolute shift in δD values, the correction itself is based on well-constrained parameters and is analytically reliable. Notably, the reference study reporting the first lunar D/H ratios by Saal et al. (2013) presented δD values that required spallation corrections ranging from 1 ‰ up to 4111 ‰, demonstrating that large correction magnitudes have been published and found trustworthy by the cosmochemistry community.

In addition, the cumulative corrections introduce a substantial associated uncertainty of approximately ±500 ‰ (2SD), which primarily affects the precision rather than the validity of the data. Before discussing the implications of these results, it is important to clarify the statistical metrics used. The standard deviation (SD) quantifies the spread of individual measurements around the mean and reflects the variability within a single sample. It is particularly useful for assessing the degree of dispersion due to measurement or natural variation. The standard error of the mean (SE), on the other hand, represents the standard deviation of the sampling distribution of the mean. It indicates how precisely the sample mean estimates the true population mean, making it especially appropriate for comparing different samples. In the context of this study, SE is the more appropriate metric as it reflects the precision of the mean hydrogen isotope value, which is central to our discussion on the similarity or difference between this sample and others from distinct parent bodies. SE also accounts for the number of replicate measurements per sample, ensuring that inter-sample comparisons are not biased by differences in the number of analyses. Although SE is typically smaller than SD, this reflects improved precision rather than an underestimation of variability. In fact, using SD alone can overstate the apparent variability due to analytical or instrumental noise, especially relevant here, given the low water content of the samples, where such variation does not reflect true natural differences. Even though the individual uncertainties on each measurement can be relatively large due to spallation correction on D/H ratios with associated extremely low water contents, the use of a weighted mean and its associated 2SE provides a statistically robust and reliable estimate of the true average composition. This approach effectively downweights less precise measurements and ensures that the final reported mean and uncertainty reflect the most probable value of the sample population. As such, the weighted mean and the standard error of the weighted mean of H_2O and δD for NWA 8409 are the most appropriate to represent its parent body, which are 3.00 ± 0.07 µg H_2O/g (2SE – only pyroxenes) and −560 ± 166 ‰ (2SE). With a MSWD value of 0.48 and a p(χ^2) of 0.87 (Figure 2), we can conclude that the nine measurements defined a single population

Table 3. δD and H_2O contents of pyroxene and olivine in NWA 8409. Standard deviations given for δD are for a Poisson distribution. δD_C is corrected for background and instrumental mass fractionation.

NWA 8409	H_2O µg/g	2SD µg/g	$\delta D_{measured}$ ‰	2SD ‰	δD_C ‰	2SD ‰	$\delta D_{spallation}$ ‰	2SD ‰
Ol1_1	2.2	0.1	196	206	176	447	−875	456
Ol1_1_re_1	1.9	0.1						
Ol1_2	2.1	0.1	612	248	745	608	−348	615
Ol1_3_1	1.5	0.1						
Ol1_4_1	1.5	0.1						
Ol2_1_1	1.8	0.1						
Ol3_1	2.3	0.2	340	209	361	479	−642	486
Cpx1_1	2.9	0.2	248	228	238	496	−556	500
Cpx1_2	2.9	0.2	366	235	394	530	−399	534
Cpx1_3	2.8	0.2	312	232	326	516	−496	521
Cpx1_4	3.1	0.2	182	206	142	439	−601	443
Cpx1_5	2.9	0.2	229	221	210	478	−585	482
Cpx1_6	3.1	0.2	396	223	417	508	−324	512
Mean (2SE)	3.0	0.3					−560	166

normally distributed around the mean. As such, the δD of −560 ± 166 ‰ (2SE) defined a reliable and precise isotopic signature of NWA 8409 parent body. To allow appropriate comparison during the discussion, all literature data used on other parent body have been reevaluated to properly calculate their weighted δD mean and standard error of the mean (2SE).

4 Discussion

The δD value of −560 ± 166 ‰ estimated for NWA 8409 is significantly lower than that of other known NC planetesimals (Figure 3a; Sarafian et al., 2019; Stephant et al., 2021), including the parent bodies of angrites (APB; Deligny et al., 2021; Rider-Stokes et al., 2024; Sarafian et al., 2017), acapulcoites-lodranites (ALPB; Stephant et al., 2023), and ordinary chondrites (Chan et al., 2021; Grant et al., 2024; Jin et al., 2021). Unlike most NC planetesimals, which are thought to have formed around 2 to 3 AU (Desch et al., 2018) at oxygen fugacities between IW−2.8 and IW+1 (Righter et al., 2016), NWA 8409 records a lower oxygen fugacity of IW−3.1 ± 0.2 (Sutton et al., 2017). Since oxygen fugacity is considered as a proxy for heliocentric distance (Rubie et al., 2015), this suggests that the parent body of NWA 8409 may have formed closer to the Sun than other NC bodies, potentially near Mercury's current orbit (∼0.4 AU). Additionally, a recent analysis found δD values as low as −850 ‰ (Aléon et al., 2022) in a CAI xenolith, suggesting a similar δD gradient across inner Solar System objects that correlated with oxygen fugacity and therefore distance (Figure 3a). These findings argue against the existence of a unique water reservoir within NC planetesimals (Stephant et al., 2023). They also challenge the notion of uniform δD background between NC and CC bodies (Grant et al., 2024) that was suggested to explain the similar δD signatures of water ice in unequilibrated ordinary chondrites (UOCs) (i.e., −370 ‰ to −70 ‰) and CCs (i.e., −400 ‰ to +100 ‰ for CV, CO, CM and CI; Piani et al., 2021). Interestingly, the δD value of bulk enstatite chondrites (ECs, i.e., 103 ± 3 ‰; Piani et al., 2020) deviates from this correlation, although recent measurements of enstatite in EH4 Indarch suggest δD = −213 ± 135 ‰ (Gruyer et al., 2024), which would make enstatite chondrites consistent with the value of −250 ‰ inferred for most NC bodies. It is important to note that bulk δD values of chondrites represent a mixture of various H-bearing components, including organics, hydrated minerals, chondrules, amorphous glasses, and unidentified components (Grant et al., 2024; Marrocchi et al., 2023; Piani et al., 2021). These components cannot be mechanically separated for measurement of their specific δD compositions (Piani et al., 2021), and caution must be taken when comparing them with differentiated objects. In achondrites, primitive achondrites, and OCs, δD values of NAMs serve as proxies for NC planetesimals δD values, whereas in ECs, bulk δD values are used. The presence of HS^-/H_2S bonding in EC chondrule mesostasis further emphasized this distinction (Thomassin et al., 2023). While the H signature of NC planetesimals is associated with H incorporated in defects within NAMs (Johnson, 2006), the H signature of ECs involves a different H speciation, that may explain why ECs deviates from the oxidation state vs. hydrogen isotope correlation shown in Figure 3a.

In terms of water abundance (Fig. 3b), we estimate a bulk water content for NWA 8409 parent body using a batch model (Peterson et al., 2023a) of 8–17 µg/g H_2O in between the estimates for the reduced aubrite parent body (< 10 µg/g; Peterson et al., 2023a), Vesta (Stephant et al., 2021), ALPB (Stephant et al., 2023) and APB (Rider-Stokes et al., 2024). It has to be noted here that the definitive quantification of parent body H_2O content is limited by our current knowledge of partition coefficients between NAMs and their parent melt. Nonetheless, the

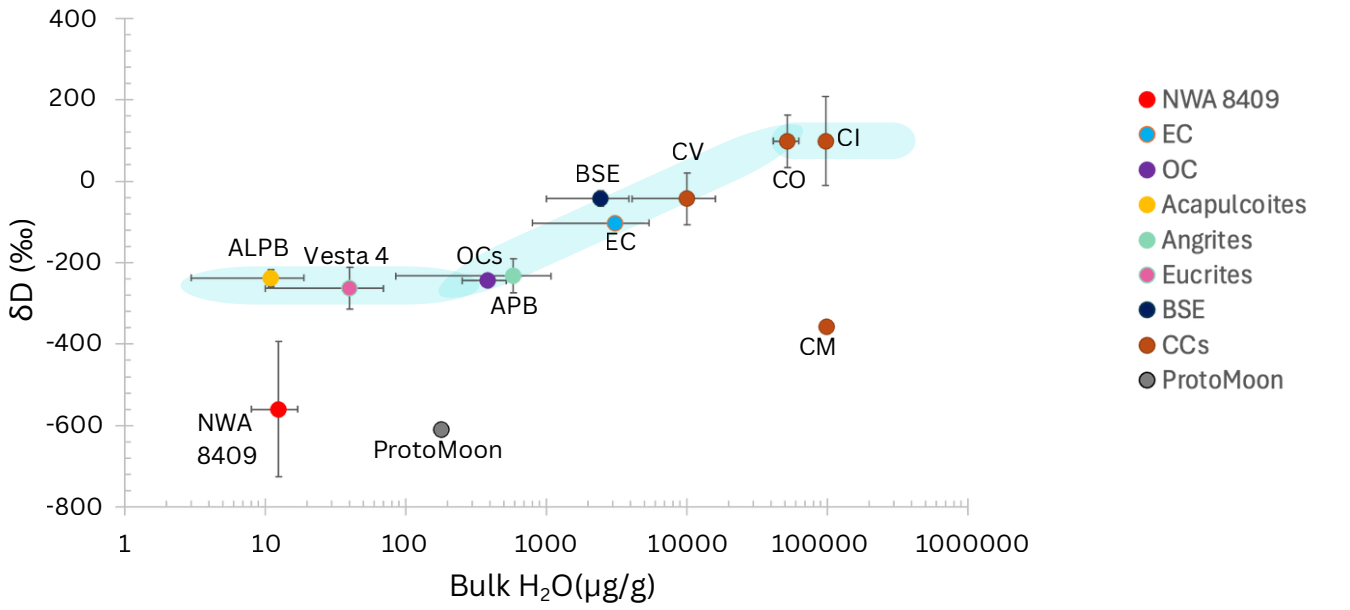

Figure 4. Bulk H_2O (in μg/g) vs. δD (in ‰) in OCs (Jin et al., 2021), ECs (Piani et al., 2020), angrites (Rider-Stokes et al., 2024), eucrites (Stephant et al., 2021), and acapulcoites-lodranites (Stephant et al., 2023) from the NC reservoir, as well as for water ice in CCs (Piani et al., 2021). The low δD ice signature of CM chondrites may result from more significant isotopic exchange, as suggested by Piani et al. (2021).

bulk water content of NC planetesimals generally correlates with their oxygen fugacity (Fig. 3b). This trend reflects not only the effect of fO_2 on H solubility (Johnson, 2006), but also additional factors: reducing planetesimals may form inside the snow line, limiting accretion of ice, and H_2 solubility in silicate melts is lower than that of H_2O (Foustoukos, 2025), further reducing their bulk H content. The high-water abundance (i.e., 0.3–0.5 wt %) in ECs (Piani et al., 2020), remains to be confirmed, as these values deviate significantly from the trend observed for other NC planetesimals, and we therefore view them with caution. Such a confirmation of high water content would again suggest that either several processes account for the H composition of the bulk enstatite chondrites, or H speciation differs from the rest of NC planetesimals.

To remove the influence of H speciation, bulk H_2O content is plotted versus bulk δD for NC planetesimals as well as for CV, CO, CM and CI chondrite water ice (Piani et al., 2021) (Figure 4). We interpret the data as follows. Because CC planetesimals (CI, CM, CR, CV) accreted at colder temperatures, they have access to a variety of H reservoirs, including interstellar water ice and organics. Generally, the trend is for more water-rich samples to have higher δD. The lower δD value for CM chondrites may reflect hydration of silicates in the nebula by H_2O vapor, as suggested for CM chondrites (Ciesla et al., 2003), which would have allowed equilibration with isotopically light nebular H_2. All NC planetesimals (including OCs, acapulcoites-lodranites, NWA 4801 angrite, eucrites, and EH4 Indarch) appear consistent with a single average value δD = −253 ± 40 ‰ (MSWD = 0.17), indicating an uniform reservoir. NWA 8409 is an exception, its δD = −560 ± 166 ‰ lying 5σ below that average. This is strong evidence that NWA 8409, NWA 7325 and paired meteorites incorporated ingassed solar nebula H_2.

Before concluding this, alternative explanations should be ruled out. The simplest interpretation is a simple mixing, in all bodies, between nebular H_2 (δD = −897 ‰) and interstellar water ice, perhaps similar to the component incorporated into the CI-type chondrite parent body (δD = +98 ± 109 ‰; Piani et al., 2021). One might surmise this simple mixing model from the roughly linear trend of δD vs. H_2O systematics seen in Figure 4 across most samples, which roughly correlates with heliocentric distance. A similar scenario of isotopic exchange between interstellar ice, sublimated water, high-temperature isotopic equilibration with nebula H_2, and/or recondensation, was suggested to explain variations among CV, CO and CI carbonaceous chondrites, with CM chondrites presumed to have equilibrated more with nebula H_2 (Piani et al., 2021). However, there are problems with this interpretation. Vesta and the ALPB deviate from this linear trend, lying above it, which would require an additional fractionation, e.g., hydrogen loss unique to those bodies. It is not clear whether ECs lie on the trend. More significantly, such a model predicts a trend like: $\delta D = +98\,‰ - 995\,‰/([H_2O]/1\,\mu g/g)$ unlike the linear trend of δD vs. $\log_{10}[H_2O]$ defined by the data. We interpret the low δD of NWA 8409 to mean that it and paired meteorites originate from a body large enough to have ingassed solar nebula H_2. For reference, a Mars-sized body (0.1 ME) is expected to retain a nebular atmosphere ~0.3 mbar (Mai et al., 2020), up to 1 bar (Stoll and Kley, 2014), while the solar nebula gas is present. A planet with a magma ocean can ingas hydrogen but is unlikely to

ingas H_2 directly, as the solubility is too low; instead, some hydrogen in a primordial atmosphere exists as or speciates to H_2O, which is then dissolved (Hirschmann et al., 2012). Assuming a solubility $xH_2O = 1300(pH_2O/1\,\text{bar})^{1/2}\,\mu g/g$ (Fricker and Reynolds, 1968) and $xH_2O = 8\,\mu g/g$, this primordial atmosphere had partial pressure of water vapor ≈ 0.037 mbar. Assuming a ratio $H_2O/H_2 = 4 \times 10^{-4}$ like the solar nebula (Lodders, 2003) we would infer $p[H_2] \approx 6$ mbar; but assuming a ratio $H_2O/H_2 \sim 0.1$ like that achievable by speciation of gas in equilibrium with a magma ocean (Hirschmann et al., 2012) at a fO_2 of ΔIW = −2 (Nicholls et al., 2024), $p[H_2] \approx 0.024$ mbar. These numbers are suggestive of a body ∼0.1 ME, the mass of proto-Mercury before the Giant Impact (Benz et al., 2007), but it is difficult to be conclusive without further modelling. Bodies this size are likely to lose gas quickly after dissipation of the nebula (Stoll and Kley, 2014), which took place early in the inner disk. This implies that the opportunity for H ingassing is therefore constrained to the brief interval during which both substantial magma oceans existed and nebular gas was still present, likely within the first 4 Ma after CAI formation (Wang et al., 2017), or possibly sooner. Formation timescales of NC bodies further support this scenario; no NC planetesimals appear to have formed after 2–2.5 Myr (Desch et al., 2018), suggesting that by the time nebular gas was dissipating, accretion in the NC region was largely complete. This is consistent with the inferred rapid early growth of Mars within a similar timeframe (Dauphas and Pourmand, 2011), reinforcing the view that early-formed, relatively large NC bodies could have transiently retained nebular atmospheres and ingassed hydrogen before gas dispersal.

5 Conclusion

While the Grand Tack model has been proposed to explain the volatile supply to growing terrestrial planets, our findings suggest this would have had limited impact on the volatile budget of precursor bodies of achondrites and primitive achondrites. Most NC bodies record a similar δD signature ∼ −250 ‰, probably inherited from a mixture of interstellar ice, similar to those in CI-type chondrites, and nebular H_2. The significantly lower δD value of NWA 8409 compared to other known NC planetesimals provides strong evidence for a distinct source of hydrogen within the early Solar System. The unique isotopic signature of NWA 8409, with its δD value of −560 ± 166 ‰, suggest that NWA 8409's parent body may have ingassed solar nebula H_2 in a manner that is not yet observed in other NC bodies, challenging the notion of a uniform water reservoir across NC and CC planetesimals and highlighting the complexity to identify the source of hydrogen in early Solar System bodies. NWA 8409 and its paired meteorites must have originated from a body large enough to retain a primordial atmosphere and incorporate hydrogen from the solar nebula. This study supports the nebular H_2 ingassing as a viable process for hydrogen incorporation, which holds significant implications for the habitability of exoplanetary systems.

Acknowledgements

We thank James Darling and Maitrayee Bose for editorial guidance and constructive comments during the review process. We also thanks the two anonymous reviewers who have contributed to improve this manuscript. Laurette Piani is thanked for their critical reading of an earlier draft of the manuscript. Kay Knight is thanked for their help with sample preparation. This research was partially founded by OI-BODIES project agreement ASI-INAF n. 2018-16-HH.0. A.S. and C.C. want to thank the support from the Italian Space Agency (ASI) within SIMBIOS-SYS project under ASI-INAF agreement 2017-47-H.0. This study was partially supported by a UK Science and Technology Facilities Council (STFC) grant to MA, IAF and BRS (#ST/T000228/1 & ST/X001180/1). Work by EF and JG was funded by the European Union (ERC, Ironis, 101087562). Views and opinions expressed are however those of the authors only and do not necessarily reflect those of the European Union or the European Research Council. Neither the European Union nor the granting authority can be held responsible for them.

Data, code, and outputs availability

Supplementary text and figures S1–S9 are available in the accompanying Supplementary Material. All raw data for NanoSIMS analyses, from both NWA 8409 and standards, are presented in the data publication of Stephant et al. (2026, https://doi.org/10.5281/zenodo.18949838). Main text figures and tables are available for download in the online version of this article.

Competing interests

The authors declare no competing interests.

References

Alexander CMO, Bowden R, Fogel ML, Howard KT, Herd CDK, Nittler LR (2012). The Provenances of Asteroids, and Their Contributions to the Volatile Inventories of the Terrestrial Planets. *Science* 337(6095): 721–723. doi:10.1126/science.1223474.

Aléon J, Lévy D, Aléon-Toppani A, Bureau H, Khodja H, Brisset F (2022). Determination of the initial hydrogen isotopic composition of the solar system. *Nature Astronomy* 6(4): 458–463. doi:10.1038/s41550-021-01595-7.

Asaduzzaman A, Muralidharan K, Ganguly J (2015). Incorporation of water into olivine during nebular condensation: Insights from density functional theory and thermodynamics, and implications for phyllosilicate formation and terrestrial water inventory. *Meteoritics & Planetary Science* 50(4): 578–589. doi:10.1111/maps.12409.

Barrat J, Greenwood R, Verchovsky A, Gillet P, Bollinger C, Langlade J, Liorzou C, Franchi I (2015). Crustal differentiation in the early solar system: Clues from the unique achondrite Northwest Africa 7325 (NWA 7325). *Geochimica et Cosmochimica Acta* 168: 280–292. doi:10.1016/j.gca.2015.07.020.

Benz W, Anic A, Horner J, Whitby JA (2007). The Origin of Mercury. *Space Science Reviews* 132(2–4): 189–202. doi:10.1007/s11214-007-9284-1.

Bischoff A, Ward D, Weber I, Morlok A, Hiesinger H, Helbert J (2013). NWA 7325—Not a typical olivine gabbro, but a rock experienced fast cooling after a second (partial) melting event. *European Planetary Science Congress* 8: EPSC2013–427. full text:EPSC2013-427.

Broadley MW, Bekaert DV, Piani L, Füri E, Marty B (2022). Origin of life-forming volatile elements in the inner Solar System. *Nature* 611(7935): 245–255. doi:10.1038/s41586-022-05276-x.

Chan QHS, Stephant A, Franchi IA, Zhao X, Brunetto R, Kebukawa Y, Noguchi T, Johnson D, Price MC, Harriss KH, Zolensky ME, Grady MM (2021). Organic matter and water from asteroid Itokawa. *Scientific Reports* 11(1). doi:10.1038/s41598-021-84517-x.

Ciesla FJ, Lauretta DS, Cohen BA, Hood LL (2003). A Nebular Origin for Chondritic Fine-Grained Phyllosilicates. *Science* 299(5606): 549–552. doi:10.1126/science.1079427.

Cleeves LI, Bergin EA, Alexander CMO, Du F, Graninger D, Öberg KI, Harries TJ (2014). The ancient heritage of water ice in the solar system. *Science* 345(6204): 1590–1593. doi:10.1126/science.1258055.

Cloutis EA, Reddy V, Blewett DT (2018). The ungrouped achondrite Northwest Africa (NWA) 7325: Spectral reflectance properties and implications for parent body identification. *Icarus* 311: 384–393. doi:10.1016/j.icarus.2018.04.027.

Dartois E, Thi WF, Geballe TR, Deboffle D, d'Hendecourt L, van Dishoeck E (2003). Revisiting the solid HDO/H$_\mathsf{2}$O abundances. *Astronomy & Astrophysics* 399(3): 1009–1020. doi:10.1051/0004-6361:20021558.

Dauphas N, Pourmand A (2011). Hf–W–Th evidence for rapid growth of Mars and its status as a planetary embryo. *Nature* 473(7348): 489–492. doi:10.1038/nature10077.

Deligny C, Füri E, Deloule E (2021). Origin and timing of volatile delivery (N, H) to the angrite parent body: Constraints from in situ analyses of melt inclusions. *Geochimica et Cosmochimica Acta* 313: 243–256. doi:10.1016/j.gca.2021.07.038.

Desch SJ, Kalyaan A, Alexander CMO (2018). The Effect of Jupiter's Formation on the Distribution of Refractory Elements and Inclusions in Meteorites. *The Astrophysical Journal Supplement Series* 238(1): 11. doi:10.3847/1538-4365/aad95f.

Desch SJ, Unterborn C, Jackson A (2022). What should meteorites from Mercury look like? *85th Annual Meeting of The Meteoritical Society* p. 6512. bibcode:2022LPICo2695.6512D.

Drake MJ (2005). Origin of water in the terrestrial planets. *Meteoritics & Planetary Science* 40(4): 519–527. doi:10.1111/j.1945-5100.2005.tb00960.x.

Foustoukos DI (2025). Molecular H2 in silicate melts. *Geochimica et Cosmochimica Acta* 389: 125–135. doi:10.1016/j.gca.2024.10.020.

Fricker PE, Reynolds RT (1968). Development of the atmosphere of Venus. *Icarus* 9(1–3): 221–230. doi:10.1016/0019-1035(68)90017-1.

Frossard P, Boyet M, Bouvier A, Hammouda T, Monteux J (2019). Evidence for anorthositic crust formed on an inner solar system planetesimal. *Geochemical Perspectives Letters* p. 28–32. doi:10.7185/geochemlet.1921.

Füri E, Deloule E, Trappitsch R (2017). The production rate of cosmogenic deuterium at the Moon's surface. *Earth and Planetary Science Letters* 474: 76–82. doi:10.1016/j.epsl.2017.05.042.

Gloeckler G, Geiss J (1998). Measurements of the abundance of Helium-3 in the Sun and in the Local Interstellar Cloud with SWICS on Ulysses. *Space Science Reviews* 84(1–2): 275–284. doi:10.1023/a:1005095907503.

Goodrich CA, Kita NT, Yin QZ, Sanborn ME, Williams CD, Nakashima D, Lane MD, Boyle S (2017). Petrogenesis and provenance of ungrouped achondrite Northwest Africa 7325 from petrology, trace elements, oxygen, chromium and titanium isotopes, and mid-IR spectroscopy. *Geochimica et Cosmochimica Acta* 203: 381–403. doi:10.1016/j.gca.2016.12.021.

Grant H, Tartèse R, Jones R, Piani L, Marrocchi Y (2024). Identification of a primordial high D/H component in the matrix of unequilibrated ordinary chondrites. *Geochimica et Cosmochimica Acta* 378: 58–70. doi:10.1016/j.gca.2024.06.005.

Gruyer C, Franchi IA, Grady MM, Anand M, Zhao X, Rider-Stokes B, Stephant A (2024). H2O abudance and H isotopic composition of nominally anhydrous mienrals from enstatite meteorites. *86th Annual Meeting of the Meteoritical Society* p. 6289. fulltext:6289.

Hirschmann M, Withers A, Ardia P, Foley N (2012). Solubility of molecular hydrogen in silicate melts and consequences for volatile evolution of terrestrial planets. *Earth and Planetary Science Letters* 345–348: 38–48. doi:10.1016/j.epsl.2012.06.031.

Hopp J, Schröter N, Pravdivtseva O, Meyer H, Trieloff M, Ott U (2018). Noble gas composition, cosmic-ray exposure age, ^{39} Ar- ^{40} Ar, and I-Xe analyses of ungrouped achondrite NWA 7325. *Meteoritics & Planetary Science* 53(6): 1150–1163. doi:10.1111/maps.13062.

Irving A, Kuehner S, Bunch T, Ziegler K, Chen G, Herd C, Conrey R, Ralew S (2013). Ungrouped mafic achondrite Northwest Africa 7325: a reduced, iron-poor cumulate olivine gabbor from a differentiated planetary parent body. *44th Lunar and Planetary Science Conference* p. 2164. bibcode:2013LPI....44.2164I.

Jin Z, Bose M, Lichtenberg T, Mulders GD (2021). New Evidence for Wet Accretion of Inner Solar System Planetesimals from Meteorites Chelyabinsk and Benenitra. *The Planetary Science Journal* 2(6): 244. doi:10.3847/psj/ac3d86.

Johnson EA (2006). Water in Nominally Anhydrous Crustal Minerals: Speciation, Concentration, and Geologic Significance. *Reviews in Mineralogy and Geochemistry* 62(1): 117–154. doi:10.2138/rmg.2006.62.6.

Kalyaan A, Desch SJ (2019). Effect of Different Angular Momentum Transport Mechanisms on the Distribution of Water in Protoplanetary Disks. *The Astrophysical Journal* 875(1): 43. doi:10.3847/1538-4357/ab0e6c.

Kleine T, Budde G, Burkhardt C, Kruijer TS, Worsham EA, Morbidelli A, Nimmo F (2020). The Non-carbonaceous–Carbonaceous Meteorite Dichotomy. *Space Science Reviews* 216(4). doi:10.1007/s11214-020-00675-w.

Koefoed P, Amelin Y, Yin QZ, Wimpenny J, Sanborn ME, Iizuka T, Irving AJ (2016). U–Pb and Al–Mg systematics of the ungrouped achondrite Northwest Africa 7325. *Geochimica et Cosmochimica Acta* 183: 31–45. doi:10.1016/j.gca.2016.03.028.

Kruijer TS, Kleine T, Borg LE (2019). The great isotopic dichotomy of the early Solar System. *Nature Astronomy* 4(1): 32–40. doi:10.1038/s41550-019-0959-9.

Kumamoto KM, Warren JM, Hauri EH (2017). New SIMS reference materials for measuring water in upper mantle minerals. *American Mineralogist* 102(3): 537–547. doi:10.2138/am-2017-5863ccbyncnd.

Leya I, Masarik J (2009). Cosmogenic nuclides in stony meteorites revisited. *Meteoritics & Planetary Science* 44(7): 1061–1086. doi:10.1111/j.1945-5100.2009.tb00788.x.

Lodders K (2003). Solar System Abundances and Condensation Temperatures of the Elements. *The Astrophysical Journal* 591(2): 1220–1247. doi:10.1086/375492.

Lécluse C, Robert F (1994). Hydrogen isotope exchange reaction rates: Origin of water in the inner solar system. *Geochimica et Cosmochimica Acta* 58(13): 2927–2939. doi:10.1016/0016-7037(94)90126-0.

Lécuyer C, Gillet P, Robert F (1998). The hydrogen isotope composition of seawater and the global water cycle. *Chemical Geology* 145(3–4): 249–261. doi:10.1016/s0009-2541(97)00146-0.

Mai C, Desch SJ, Kuiper R, Marleau GD, Dullemond C (2020). The Dynamic Proto-atmospheres around Low-mass Planets with Eccentric Orbits. *The Astrophysical Journal* 899(1): 54. doi:10.3847/1538-4357/aba4a8.

Marrocchi Y, Rigaudier T, Piralla M, Piani L (2023). Hydrogen isotopic evidence for nebular pre-hydration and the limited role of parent-body processes in CM chondrites. *Earth and Planetary Science Letters* 611: 118151. doi:10.1016/j.epsl.2023.118151.

McCubbin FM, Barnes JJ (2019). Origin and abundances of H2O in the terrestrial planets, Moon, and asteroids. *Earth and Planetary Science Letters* 526: 115771. doi:10.1016/j.epsl.2019.115771.

Morbidelli A, Bitsch B, Crida A, Gounelle M, Guillot T, Jacobson S, Johansen A, Lambrechts M, Lega E (2016). Fossilized condensation lines in the Solar System protoplanetary disk. *Icarus* 267: 368–376. doi:10.1016/j.icarus.2015.11.027.

Newcombe ME, Nielsen SG, Peterson LD, Wang J, Alexander CMO, Sarafian AR, Shimizu K, Nittler LR, Irving AJ (2023). Degassing of early-formed planetesimals restricted water delivery to Earth. *Nature* 615(7954): 854–857. doi:10.1038/s41586-023-05721-5.

Nicholls H, Lichtenberg T, Bower DJ, Pierrehumbert R (2024). Magma Ocean Evolution at Arbitrary Redox State. *Journal of Geophysical Research: Planets* 129(12). doi:10.1029/2024je008576.

Olson P, Sharp ZD (2018). Hydrogen and helium ingassing during terrestrial planet accretion. *Earth and Planetary Science Letters* 498: 418–426. doi:10.1016/j.epsl.2018.07.006.

O'Brien DP, Izidoro A, Jacobson SA, Raymond SN, Rubie DC (2018). The Delivery of Water During Terrestrial Planet Formation. *Space Science Reviews* 214(1). doi:10.1007/s11214-018-0475-8.

Peslier AH, Schönbächler M, Busemann H, Karato SI (2017). Water in the Earth's Interior: Distribution and Origin. *Space Science Reviews* 212(1–2): 743–810. doi:10.1007/s11214-017-0387-z.

Peterson LD, Newcombe ME, Alexander CM, Wang J, Klein F, Bekaert DV, Nielsen SG (2023a). The H content of aubrites: An evaluation of bulk versus in situ methods for quantifying water in meteorites. *Earth and Planetary Science Letters* 620: 118341. doi:10.1016/j.epsl.2023.118341.

Peterson LD, Newcombe ME, Alexander CM, Wang J, Nielsen SG (2024). The H-poor nature of incompletely melted planetesimals: The view from acapulcoites and lodranites. *Geochimica et Cosmochimica Acta* 370: 1–14. doi:10.1016/j.gca.2024.02.002.

Peterson LD, Newcombe ME, Alexander CMO, Wang J, Sarafian AR, Bischoff A, Nielsen SG (2023b). The H2O content of the ureilite parent body. *Geochimica et Cosmochimica Acta* 340: 141–157. doi:10.1016/j.gca.2022.10.036.

Piani L, Marrocchi Y, Rigaudier T, Vacher LG, Thomassin D, Marty B (2020). Earth's water may have been inherited from material similar to enstatite chondrite meteorites. *Science* 369(6507): 1110–1113. doi:10.1126/science.aba1948.

Piani L, Marrocchi Y, Vacher LG, Yurimoto H, Bizzarro M (2021). Origin of hydrogen isotopic variations in chondritic water and organics. *Earth and Planetary Science Letters* 567: 117008. doi:10.1016/j.epsl.2021.117008.

Raymond SN, Izidoro A (2017). Origin of water in the inner Solar System: Planetesimals scattered inward during Jupiter and Saturn's rapid gas accretion. *Icarus* 297: 134–148. doi:10.1016/j.icarus.2017.06.030.

Rider-Stokes B, Stephant A, Anand M, Franchi I, Zhao X, White L, Yamaguchi A, Greenwood R, Jackson S (2024). Evidence against water delivery by impacts within 10 million years of planetesimal formation. *Earth and Planetary Science Letters* 642: 118860. doi:10.1016/j.epsl.2024.118860.

Righter K, Sutton SR, Danielson L, Pando K, Newville M (2016). Redox variations in the inner solar system with new constraints from vanadium XANES in spinels. *American Mineralogist* 101(9): 1928–1942. doi:10.2138/am-2016-5638.

Rubie D, Jacobson S, Morbidelli A, O'Brien D, Young E, de Vries J, Nimmo F, Palme H, Frost D (2015). Accretion and differentiation of the terrestrial planets with implications for the compositions of early-formed Solar System bodies and accretion of water. *Icarus* 248: 89–108. doi:10.1016/j.icarus.2014.10.015.

Saal AE, Hauri EH, Van Orman JA, Rutherford MJ (2013). Hydrogen Isotopes in Lunar Volcanic Glasses and Melt Inclusions Reveal a Carbonaceous Chondrite Heritage. *Science* 340(6138): 1317–1320. doi:10.1126/science.1235142.

Sarafian AR, Nielsen SG, Marschall HR, Gaetani GA, Hauri EH, Righter K, Sarafian E (2017). Angrite meteorites record the onset and flux of water to the inner solar system. *Geochimica et Cosmochimica Acta* 212: 156–166. doi:10.1016/j.gca.2017.06.001.

Sarafian AR, Nielsen SG, Marschall HR, Gaetani GA, Righter K, Berger EL (2019). The water and fluorine content of 4 Vesta. *Geochimica et Cosmochimica Acta* 266: 568–581. doi:10.1016/j.gca.2019.08.023.

Shimizu K, Alexander CM, Hauri EH, Sarafian AR, Nittler LR, Wang J, Jacobsen SD, Mendybaev RA (2021). Highly volatile element (H, C, F, Cl, S) abundances and H isotopic compositions in chondrules from carbonaceous and ordinary chondrites. *Geochimica et Cosmochimica Acta* 301: 230–258. doi:10.1016/j.gca.2021.03.005.

Stephant A, Desch S, Anand M, Zhao X, Cuppone T, Rider-Stokes BG, Gamblin J, Füri E, Nottingham M, Carli C, Franchi I, Pratesi G (2026). Petrographic, Geochemical, Isotopic, and Noble Gas Characterization of NWA 8409. Version v6. Zenodo. doi:10.5281/zenodo.18949838.

Stephant A, Wadhwa M, Hervig R, Bose M, Zhao X, Barrett T, Anand M, Franchi I (2021). A deuterium-poor water reservoir in the asteroid 4 Vesta and the inner solar system. *Geochimica et Cosmochimica Acta* 297: 203–219. doi:10.1016/j.gca.2021.01.004.

Stephant A, Zhao X, Anand M, Davidson J, Carli C, Cuppone T, Pratesi G, Franchi I (2023). Hydrogen in acapulcoites and lodranites: A unique source of water for planetesimals in the inner Solar System. *Earth and Planetary Science Letters* 615: 118202. doi:10.1016/j.epsl.2023.118202.

Stoll MHR, Kley W (2014). Vertical shear instability in accretion disc models with radiation transport. *Astronomy & Astrophysics* 572: A77. doi:10.1051/0004-6361/201424114.

Sutton S, Goodrich C, Wirick S (2017). Titanium, vanadium and chromium valences in silicates of ungrouped achondrite NWA 7325 and ureilite Y-791538 record highly-reduced origins. *Geochimica et Cosmochimica Acta* 204: 313–330. doi:10.1016/j.gca.2017.01.036.

Tartèse R, Anand M, Franchi IA (2019). H and Cl isotope characteristics of indigenous and late hydrothermal fluids on the differentiated asteroidal parent body of Grave Nunataks 06128. *Geochimica et Cosmochimica Acta* 266: 529–543. doi:10.1016/j.gca.2019.01.024.

Thomassin D, Piani L, Villeneuve J, Caumon MC, Bouden N, Marrocchi Y (2023). The high-temperature origin of hydrogen in enstatite chondrite chondrules and implications for the origin of terrestrial water. *Earth and Planetary Science Letters* 616: 118225. doi:10.1016/j.epsl.2023.118225.

Vermeesch P (2018). IsoplotR: A free and open toolbox for geochronology. *Geoscience Frontiers* 9(5): 1479–1493. doi:10.1016/j.gsf.2018.04.001.

Wang H, Weiss BP, Bai XN, Downey BG, Wang J, Wang J, Suavet C, Fu RR, Zucolotto ME (2017). Lifetime of the solar nebula constrained by meteorite paleomagnetism. *Science* 355(6325): 623–627. doi:10.1126/science.aaf5043.

Weber I, Morlok A, Bischoff A, Hiesinger H, Ward D, Joy KH, Crowther SA, Jastrzebski ND, Gilmour JD, Clay PL, Wogelius RA, Greenwood RC, Franchi IA, Münker C (2016). Cosmochemical and spectroscopic properties of Northwest Africa 7325—A consortium study. *Meteoritics & Planetary Science* 51(1): 3–30. doi:10.1111/maps.12586.

Wu J, Desch SJ, Schaefer L, Elkins-Tanton LT, Pahlevan K, Buseck PR (2018). Origin of Earth's Water: Chondritic Inheritance Plus Nebular Ingassing and Storage of Hydrogen in the Core. *Journal of Geophysical Research: Planets* 123(10): 2691–2712. doi:10.1029/2018je005698.

Yang J, Lin Y, Changela H, Xie L, Chen B, Yang J (2020). Early sulfur-rich magmatism on the ungrouped achondrite Northwest Africa 7325 differentiated parent body. *Meteoritics & Planetary Science* 55(9): 1951–1978. doi:10.1111/maps.13559.

Yang X, Keppler H, Li Y (2016). Molecular hydrogen in mantle minerals. *Geochemical Perspectives Letters* 2: 160–168. doi:10.7185/geochemlet.1616.

Zimmermann L, Füri E, Boulliung J, Saxton JM (2025). Performance of the 3F4M Noblesse–HR Noble Gas Mass Spectrometer for Multicollection Ne-Ar-N_2 Analyses. *Geochemistry, Geophysics, Geosystems* 26(7). doi:10.1029/2025gc012247.